ASSESSING AND IMPROVING CURRENT EFFICIENCY IN MAGNESIUM BASE SACRIFICIAL ANODES BY MICROSTRUCTURE CONTROL

J. Genescá*, C. Rodriguez

Departamento Ingeniería Metalúrgica. Facultad Quimica. UNAM. Ciudad Universitaria. 04510 Mexico D.F.

J.Juarez
Instituto Investigación en Materiales. UNAM. Ciudad Universitaria. 04510 México D.F.

and

B. Campillo, L. Martinez
Lab. Cuernavaca. IFUNAM. P.O. Box 48-3. 62251 Cuernavaca, Mor., México

ABSTRACT

To investigate the main reasons for low current efficiency of the commercial magnesium sacrificial anodes, a study was carried out with the main objective of correlating the microstructure characteristics and the alloying elements of the magnesium anodes with their efficiency.

Several heat treatments were performed and the anodic efficiency was determined. An increase of 10 to 12% of the efficiency was obtained. The increments in the efficiency were related to the microstructural characteristics and the appearance of second phase particles influences the form of corrosion process exhibited.

An electrochemical evaluation was carried out in order to gain a deeper understanding of magnesium corrosion by using transient electrochemical measurements.

* To whom all correspondence should be addressed

Keywords: magnesium sacrificial anodes, efficiency, microstructure control, heat treatments, EIS.

INTRODUCTION

Applications of Mg sacrificial anodes for cathodic protection (CP) of underground pipelines are well known. In the case of Mexico there are approximately 59,000 km of pipes distributed throughout the country. The amount of Mg anodes employed to protect this infrastructure is very high.

In recent years a controversy has sprung up in Mexico related to the low current efficiency of commercial magnesium anodes and their electrochemical evaluation. Two standards are applied in this evaluation: ASTM G - 97 - 89 /1/ and NOM K 109 - 1977 /2/. The differences between both standards are summarized in Table I, and mainly are: the current density (0.039 mA/cm^2 in ASTM and 1.25 mA/cm^2 in Mexican standard), testing period (14 days and 4-5 days) and the electrolyte ($CaSO_4.2H_2O$ + $Mg(OH)_2$ and synthetic sea water).

The problems of low current efficiency are generally due to the nature of the alloying elements, purity of Mg and microstructure. Small changes in composition and heat treatment can affect the corrosion behaviour of the alloy substantially. However, characterization of the alloy anodes in relation to such changes is lacking in the literature.

The effect of surface inhomogeneities in corrosion processes and the resulting localized corrosion attack are usually investigated *ex situ* by microscopic and surface analytical techniques.

Mg anodes currently have limited offshore use. Alloys of Mg are particularly suited for high resistivity environments where their inherent negative potential and high current output per unit weight are desirable. The theoretical half-cell potential of magnesium is -2.37 V vs. NHE or -2.12 V vs. SCE. However, the practical measured potential of a magnesium anode is considerably more noble. The AZ63A anode (nominal 6% Al and 3% Zn) has a potential of -1.48 V vs. SCE, while the proprietary Galvomag anode containing high purity magnesium with 0.9 - 1.2% added Mn and controlled impurities has a solution potential of -1.68 vs. SCE.

Aside from the large difference observed between theoretical and measured solution potentials, magnesium anodes generally have a current efficiency less than other galvanic anodes. The theoretical current yield of a

Table I
Main differences between ASTM G-97-89 and NOM K-109-1977 standards

CONDITIONS	ASTM G-97-89	NOM K-109-1977
Anode Magnesium cylinder	l = 15.20 cm dia. = 1.27 cm	l = 8.0 cm dia. = 1.6 cm
Anode area	41.2 cm^2	42.2 cm^2
Cathode	steel pipe l = 16.5 cm dia. = 7.62 cm	mesh steel cylinder
Electrochemical cell	same steel pipe employed as cathode	glass container l = 17 cm dia. = 12.0 cm volume 1600 cm^3
Current density,	0.039 mA/cm^2	1.25 mA/cm^2
Testing period	14 days	4 to 5 days
Electrolyte	$CaSO_4.2H_2O$ 5.0 g/l $Mg(OH)_2$ 0.1 g/l	Synthetic sea water ASTM D1141-75
Anode cleaning solution	CrO_3 250 g/l 30 minutes	Ag_2CrO_4.....1 % CrO_3.....15 % 1-3 minutes. Boiling temp.

magnesium anode is approximately 2200 A-h/Kg (1000 A-h/lb.). The practically observed current efficiency rarely exceeds 50-60%.

At least three areas are known to contribute to the factors responsible for the low current efficiency and more-noble-than theoretical solution potential of the magnesium anode /3/:

1. Anolyte chemistry - changes in anion and cation concentration which occur close to the dissolving magnesium surface and the effect that these ions have on behaviour.
2. Anode alloying elements and structure - alloying elements and thermal story attendant with casting affect the structure which are in turn related to filming characteristics and local-cell action.
3. Anodic electrochemistry.

Nowadays, the increasing demand for cathodic protection of domestic and industrial structures and also installed equipment has given rise to widespread interest in new developments and applications of galvanic anodes. Important work has been done to improve the most important properties of galvanic anodes through considerations of metal purity /4/, alloying /5,6/ and backfill material /7/. Also a great deal of attention has been paid to improvements in current efficiency, polarization characteristics and the distribution of corrosion attack at the anodes.

Anode solution potential is significantly important, for instance, in high resistivity soils where the cathodic structure is relatively inaccessible. The extra driving force afforded by a high potential anode is specially desirable. In normal soils, an anode with increased potential would bring decreases in installation costs since fewer anodes would be required to satisfy the current requirements of a particular structure.

Studies concerning the factors responsible for the low current efficiency in magnesium anodes included changes in anion and cation concentration which occur close to the dissolving magnesium surface and the anodic electrochemistry have been carried out in the past /3,6,7/.

The composition of a magnesium anode is known to affect its current capacity, solution potential and efficiency. Many alloying elements have been used in order to improve the properties of magnesium anodes. The primary alloying elements aluminium and zinc have an insignificant effect in the ranges ordinarily specified. Iron levels as low as 0.035% are tolerated at manganese contents in excess of 0.2% without an efficiency sacrifice. Lower iron concentrations with correspondingly lower manganese are desired and should be the practical casting consideration, adverse current capacity results from low (0.05%) copper contents. Manganese is an excellent alloying element in magnesium alloys for control of impurities, particularly iron and also appears partially to offset the effect of copper in the AZ63 alloy. Nickel can adversely affect anode efficiency at levels down to 0.0005% in these alloys. For good grade anode material, a nickel maximum of 0.002% is permitted if efficiencies are to be above 50%. The key to the performance of the high purity magnesium alloys lies in the metallurgical state of the alloy itself /5/. Care must be given to the distribution of iron between magnesium-rich and copper-rich phases present in the alloy.

On the other hand, a significant amount of Mexican consumers of magnesium-based sacrificial anodes (most of whom are involved in the

Mexican national pipeline system) are concerned with respect to the casting procedures and cathodic-protection efficiency. Cathodic protection is now a well-established activity and there are widespread compulsory requirements for pipeline protection. There is, therefore, current interest in improving magnesium anodes.

It has been pointed out in the past that the metallurgical features of Mg sacrificial anodes such as casting conditions and heat treatment are closely related to the anode operation potential and also to their own efficiency. In the magnesium type of anodes, contrary to the requirements for anode materials, the corrosion occurs by pitting rather than by uniform corrosion. This corrosion characteristics shifts the potential to more electronegative values /8/. For instance, magnesium suffers pitting when it is exposed to chloride solutions in nonoxidizing media at open circuit potentials /9/. The deleterious effects of Ni, Fe and Cu in magnesium anodes are well documented /10/.

PURPOSE

In order to investigate the main reasons for low current efficiency of the normal commercial magnesium sacrificial anodes, a study was carried out with the main objective of correlating the microstructure characteristics and the alloying elements of the magnesium anodes with their efficiency under operating field conditions. Also, heat treatment effects on the current efficiency of commercial Mg anodes has been studied.

Additionally, an electrochemical evaluation was carried out in order to gain a deeper understanding of magnesium corrosion by using transient electrochemical measurements.

Effect of Microstructure Characteristics and Alloying Elements

Experimental Procedure

Commercial magnesium of chemical composition shown in Table II was induction melted under an argon atmosphere in a steel crucible. The temperature of the bath was monitored using a chromel/alumel thermocouple. When temperature reached 50°C of superheat, the power unit was cut off and the melt was gravity casting under an argon atmosphere into cylindrical copper mould (25 mm inside diameter and 60 mm outside

Table II
Chemical analysis of commercial magnesium (wt%)

Material	Al	Cu	Ni	Fe	Mn	Mg
As received	2.0	0.0004	0.003	0.043	1.0	bal.
As cast	1.8	0.0004	0.003	0.030	0.2	bal.

diameter, 110 mm long). The amount of superheat was controlled in order to avoid excessive shrinkage. Samples for chemical analyses were taken from the top and bottom of each ingot. The chemical analyses of the ingots are included in Table II.

Specimens were cut off, ground from 80 to 600 grit and polished on 1 μm alumina lap wheels. The polished specimens were ultrasonically cleaned, dried and etched with 1% oxalic acid in water. Micrographs of representative areas were taken in an Olympus PMG3 optical and a Jeol 6400 scanning electron microscopes.

To assess the effect of heat treatment on the cast magnesium ingots, the specimens were heat treated at 300°C for 8 hours under an argon atmosphere. Microanalyses of the sacrificial anodes with and without heat treatment were carried out in the scanning electron microscope.

Cylindrical anodes 20 mm in diameter and 80 mm high were machined from the magnesium ingots with and without heat treatment. Electrochemical evaluation was carried out according to ASTM G97-89 with the standard laboratory test method for magnesium sacrificial anodes for underground applications /1/.

Results and Discussion

Figure 1 shows a micrograph of the structure obtained by gravity casting of commercial magnesium into a copper mould. As can be observed, the microstructure in all the ingots was of the cellular type. Cell size in ingots varied between 5 μm in the centre of the ingot to above 10 μm in the outer region of the ingot. The microstructure mainly consists of cells of α-Mg, but few precipitates were observed at cell boundaries. Because the magnesium ingots were produced in order to assess their behaviour as magnesium sacrificial anodes, a heat treatment was performed at 300°C for eight hours.

Fig. 1: Cellular microstructure obtained by gravity casting commercial magnesium into a cylindrical copper mould. Second phase particles were detected as Fe-rich particles.

Figure 2 shows the microstructure observed in all the specimens, which consists mainly of equiaxed grains, inside these grains a cellular structure was observed and these cells were nearly free of precipitates.

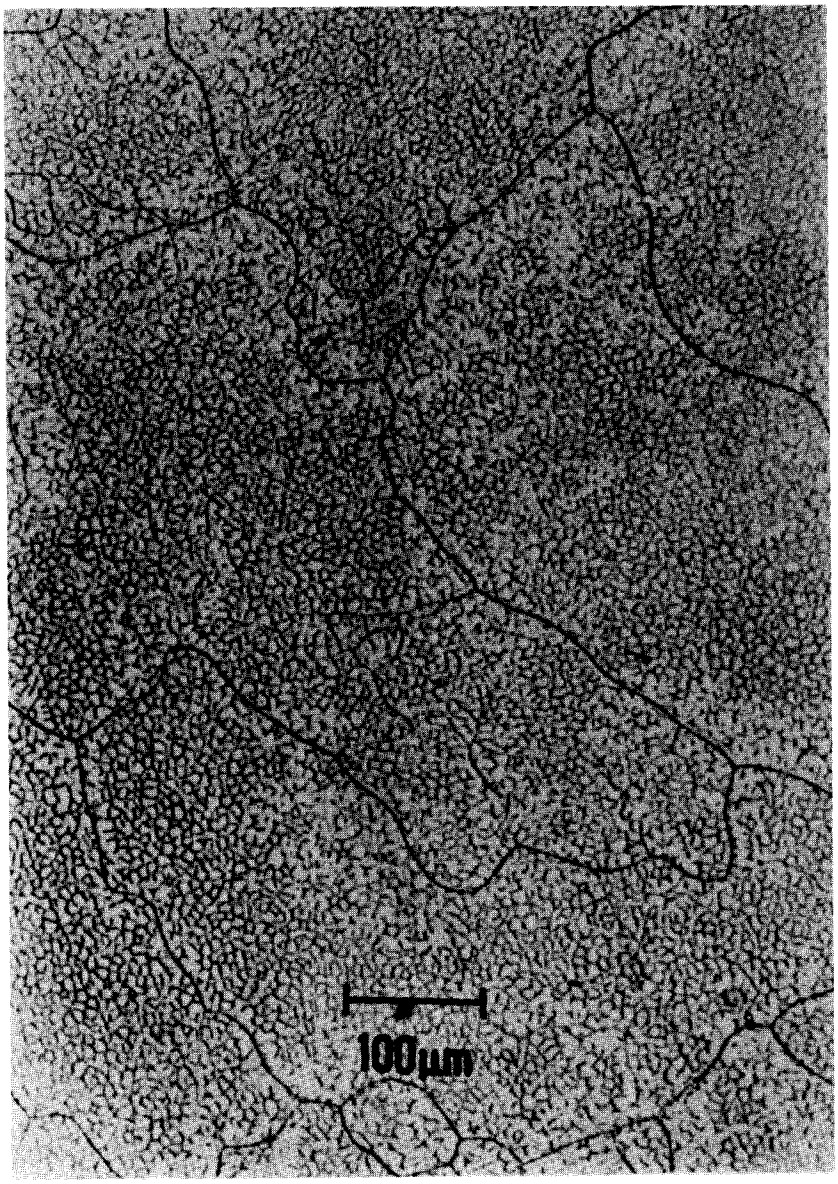

Fig. 2: Equiaxed grain structure of a magnesium sacrificial anode after heat treatment (300°C, 8 hrs). Inside the equiaxed grains, a cellular microstructure is observed with nearly free precipitates.

Microanalyses were carried out in order to quantify how the microstructure was modified by the chill casting technique and the heat treatment of specimens, before performing the evaluation of magnesium sacrificial anode test for underground applications, in terms of the nature of impurities such as copper, iron and nickel.

In the as-cast magnesium ingots and specially in regions where the precipitates were present, the microanalysis system detected precipitates rich in iron (shown in Figure 1) and a uniform concentration of copper, iron and nickel in solid solution with some major concentration of iron at grain boundaries.

Microanalyses of the magnesium ingots with heat treatment revealed small random iron-rich precipitates and a layer of aluminium-rich second phase of about 0.05 μm in thickness was detected at grain boundaries.

Table III shows the initial and final weights of the sacrificial anode test specimens with and without heat treatment. Values for the anode efficiency and closed and open circuit potential measured for each test specimen are also included. The efficiency values for the sacrificial anode specimen in the as cast condition are superior to 50% and with heat treatment, the efficiency values are close to 70%.

After evaluation of the magnesium sacrificial anode test, the surface of specimens was observed. Figure 3 shows the microstructure of magnesium in the as-cast condition after evaluation of its efficiency. As can be seen, corrosion of magnesium occurs preferentially in regions rich in second

Table III
Current efficiency of sacrificial anode test specimens

Anode	Initial weight (g)	Final weight (g)	Weight loss (g)	Efficiency (%)	Circuit potential (mV) vs sce	
					open	closed
As cast	24.73535	24.3658	0.36955	52.3	-1,520	-1,514
Heat treated	24.78035	24.49710	0.28325	68.6	-1,468	-1,471

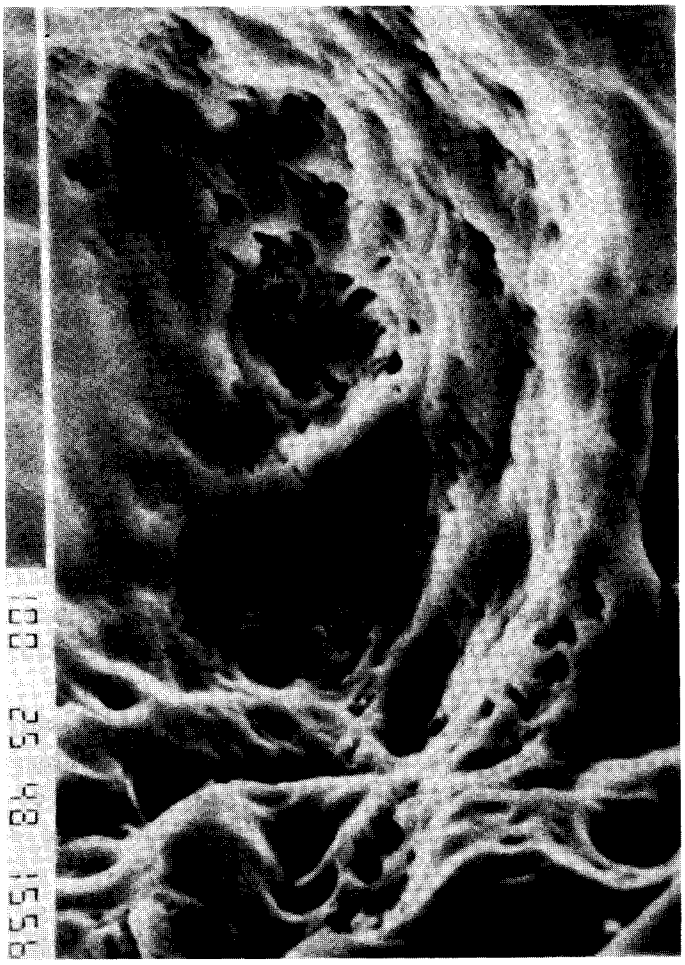

Fig. 3: Microstructure of magnesium in the as-cast condition after the evaluation test, in which it can be observed that the corrosion pattern is by pitting.

phase Fe-rich precipitates, which were located at cell boundaries. Corrosion in these regions is by pitting, forming a step-like pattern.

Figure 4 shows the observed microstructure of the magnesium sacrificial anode with heat treatment after the test. The corrosion features are more uniformly distributed compared to specimens without heat treatment, and corrosion was of the uniform type.

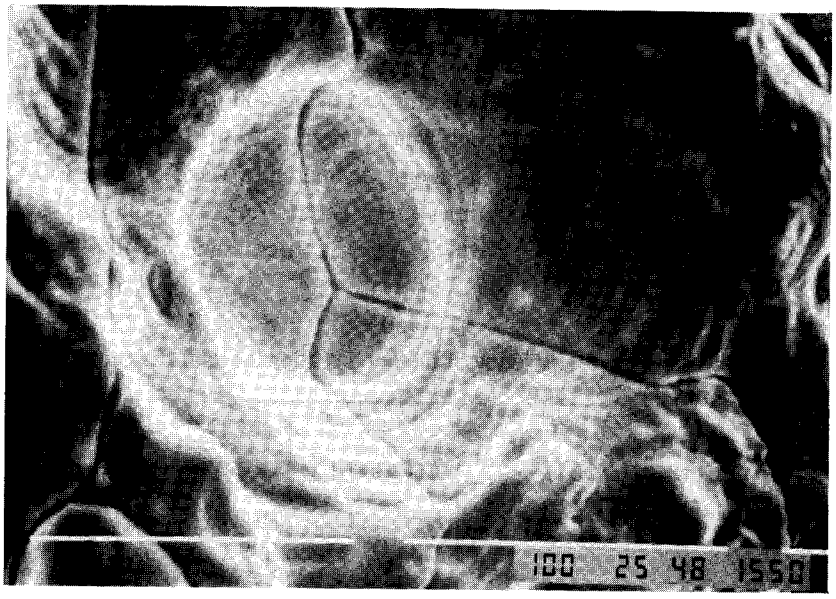

Fig. 4: Microstructure of magnesium in the as-heat treated condition after the evaluation test. Corrosion is more uniform as compared to the as-cast magnesium.

Heat Treatment Effects on Commercial Mg Anodes

Experimental Procedure

A commercial magnesium anode of bulk chemical composition (in wt%): 0.012 % Cu, 0.056 %Fe, 1.260 %Mn, 0.007 %Ni and 0.004 %Al and Mg bal., was used for the present work. The chemical analysis was performed according to the ASTM standard /1/. From the composition it is clear that the Fe value is high compared to the typical value of 0.03% reported for these type of anodes, Table VI. Also the Ni content is above of the typical value of 0.001%. Several cuttings were performed according to ASTM G 97-89 /1/ in order to obtain cylindrical anodes. The dimensions of the test anodes were 152x12.7 mm and special care during their machining was necessary in order to avoid heating. These anodes were lapped to a 240 grit finish and thoroughly cleaned and weighed, before the electrochemical evaluation was carried out. In order to assess the effect of heat treatments on the commercial anode, using the same specimens obtained for the ASTM tests, several cooling rates were used (i.e.50, 400 and 1000 $^{\circ}$C/sec.) under an

argon atmosphere, using several holding times at temperature. The heating temperature was 400°C, and from this all the cooling rates were carried out. Also, two ageing treatments were performed using 400°C and 300°C as the solution temperatures at different times ranging from 1.8 to 57.6 Ks, followed by a water quench. The ageing temperature was 250 and 150°C respectively at different holding times (from 1.8 to 57.6 Ks.).Table IV shows all the thermal treatments which were carried out in this work.

Table IV

Electrochemical efficiency of the anodes after thermal treatments

CONDITION	EFFICIENCY (%) †	Open Circuit Potential‡, mV vs sce	Closed Circuit Potential, mV vs sce
As - cast	45.73	-1686	-1558
Furnace cooled (≈50°C/s), 400°C/18 Ks	30.42	-1499	-1478
Furnace cooled (≈50°C/s), 400°C/28.8 Ks	26.53	-1591	-1581
Furnace cooled (≈50°C/s), 400°C/57.6 Ks	25.78	-1600	-1572
Cooled in air (≈400°C/s), 400°C/18 Ks	42.03	-1714	-1497
Cooled in air (≈400°C/s), 400°C/28.8 Ks	10.42	-1584	-1568
Cooled in air (≈400°C/s), 400°C/57.6 Ks	8.99	-1620	-1595
Solution Treated 400°C/1.8 Ks, water cooled (≈1000°C/s), aged 150°C/1.8 Ks	47.5	-1517	-1576
Solution Treated 400°C/18 Ks, water cooled (≈1000°C/s), aged 250°C/18 Ks	23.5	-1713	-1585
Solution Treated 400°C/28.8 Ks, water cooled (≈1000°C/s), aged 250°C/28.8 Ks	33.05	-1777	-1590
Solution Treated 400°C/57.6 Ks, water cooled (≈1000°C/s), aged 250°C/57.6 Ks	22.98	-1789	-1550
Solution Treated 300°C/1.8 Ks, water cooled (≈1000°C/s), aged 150°C/1.8 Ks	52.77	-1495	-1483
Solution Treated 300°C/18 Ks, water cooled (≈1000°C/s), aged 150°C/18 Ks	60.77	-1614	-1503
Solution Treated 300°C/28.8 Ks, water cooled (≈1000°C/s), aged 150°C/28.8 Ks	63.85	-1661	-1480
Solution Treated 300°C/57.6 Ks, water cooled (≈1000°C/s), aged 150°C/57.6 Ks	56.43	-1492	-1482

†These values represent an average for 5 test specimens

‡These represent an average value of the circuit potential

Metallographic specimens were prepared and photomicrographs were taken with both an optical and a scanning electron microscope equipped with an energy dispersive X-ray spectrometer. The sacrificial anodes with and without heat treatment were evaluated electrochemically according to ASTM G 97-89 /1/ with the standard laboratory test method for magnesium sacrificial anodes for underground applications. For this test, a known direct current is passed through a test cell connected in series (galvanostatic method). Each test cell consists of a preweighed magnesium anode specimen, a steel pot container, and a solution of $CaSO_4$ +$Mg(OH)_2$. The specimens oxidation potential is measured several times during the 14 day/test and one hour after the current is turned off. At the conclusion of the test, each specimen is cleaned and weighed. The ampere-hours obtained per unit mass of specimen lost are calculated. The values obtained are shown in Table IV; these values represent an average from 5 test samples. Also, the closed and open circuit potential average values are shown. After assessment of the current efficiency, the specimens were observed under a scanning electron microscope (SEM) at 25 kV.

Results and Discussion

Figure 5 shows a micrograph of the microstructure of the anode in the as-received condition. As can be observed, the microstructure shows columnar grains, and inside of the columnar grains a substructure is formed constituted by equiaxed grains. The size being approximately of 100μm, in

Table V

Microstructural parameters of the Mg anodes after thermal treatments

Condition	Columnar grain size (range, μm)	Particle size (range, μm)	Morphology	Elements detected by EDAX
as-cast	100-160	10-12	spherical-irregular	Fe-Mn (Fe rich)
air-cooled	120-180	8-9	spherical-irregular	Fe-Mn
furnace-cooled	120-200	8-10	spherical	Fe-Mn
aged	180-250	1-3	spherical	Mg-Al, Fe-Mn

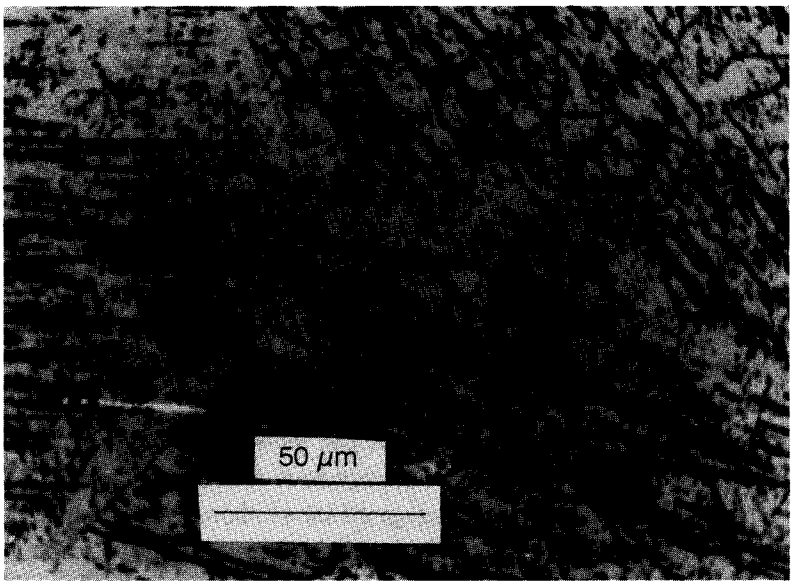

Fig. 5a: Microstructure of the anode in the as-received condition.

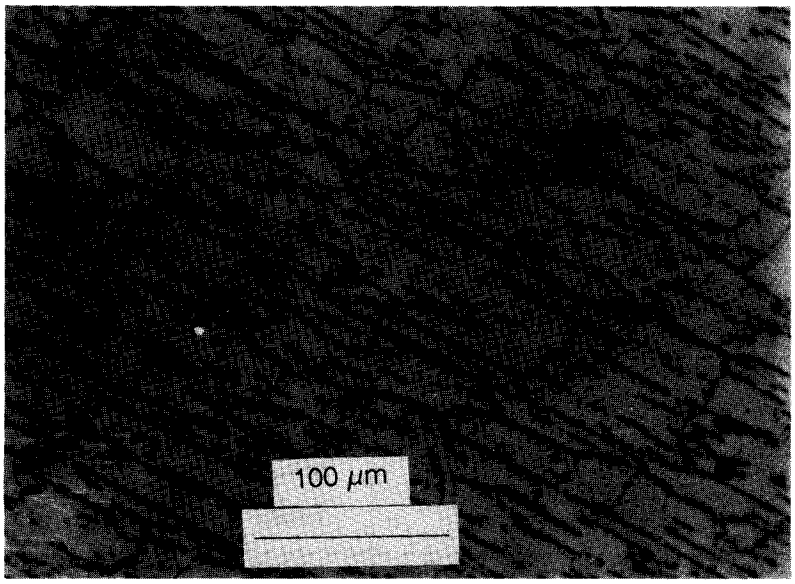

Fig. 5b: Detail of the microstructure on the anode in the as-received condition.

the centre of the anode (Figure 5a). The microstructure mainly consists of columnar grains of α-Mg. Few precipitates were observed at the interior of the columnar grains at the equiaxed grains and at the grain boundaries (Figure 5b). The microanalysis detected that the precipitates observed were mainly rich in Fe and Mn (similar to the inset EDAX pattern in Figure 6a). The heat treatments carried out in the as-cast anodes modified substantially the microstructure and the microanalysis of the precipitates. Figure 6a shows a micrograph obtained when the as-cast anode was heat treated and cooled in air, showing columnar type structure with a substructure inside these columnar grains with very fine precipitates, but these precipitates are concentrated near the grain boundaries. Microanalysis indicate the presence of Fe and Mn in these fine precipitates, and relatively high concentration of Mn being segregated as a second phase particle (the diagram is shown in the inset). Figure 6b is the microstructure obtained from the anode being solution treated at 300°C and then aged during 28.8 Ks at 150°C. It shows a needle-like structure associated with very fine precipitates, finely distributed in the matrix, and in these precipitates the microanalysis showed the presence of Fe, Mn, Mg and Al (the diagram is shown in the inset). The formation of Al and Mg particles at the grain boundaries, indicates that this treatment may have redissolved the Fe-Mn particles to form Mn rich second phase particles. Figure 7 shows the % efficiency as a function of treatment time for the two ageing treatments used in this work (300°C and 400°C). The efficiency increases with treatment time up to 28.8 Ks. After this time is reached the efficiency decreases which corresponds to the formation of Fe-Mn particles, a co-precipitation process, localized mainly at the grain boundaries. Fe-Mn particles induce the formation of microcells where the corrosion is localized .

Table V shows a summary of the main microstructural parameters being observed and measured for the different heat treatments carried out. Table IV shows the efficiency values obtained. Notice that the efficiency increases as the particle size tends to decrease, specifically for ageing treatments at 300°C. The morphology changes to spherical and the chemistry of these particles changes with the formation of an Al-Mg compound at the grain boundaries which helps to obtain a higher efficiency. This behaviour may be due to the Al-Mg compounds at the grain boundaries acting as-local cathodes with respect to the matrix. It has been reported that the benefit of Al is likely related to the nature of Mg-Al-oxide (Mg-rich) which is thinner with increasing Al content /11/. Also there is a strong tendency for Al to

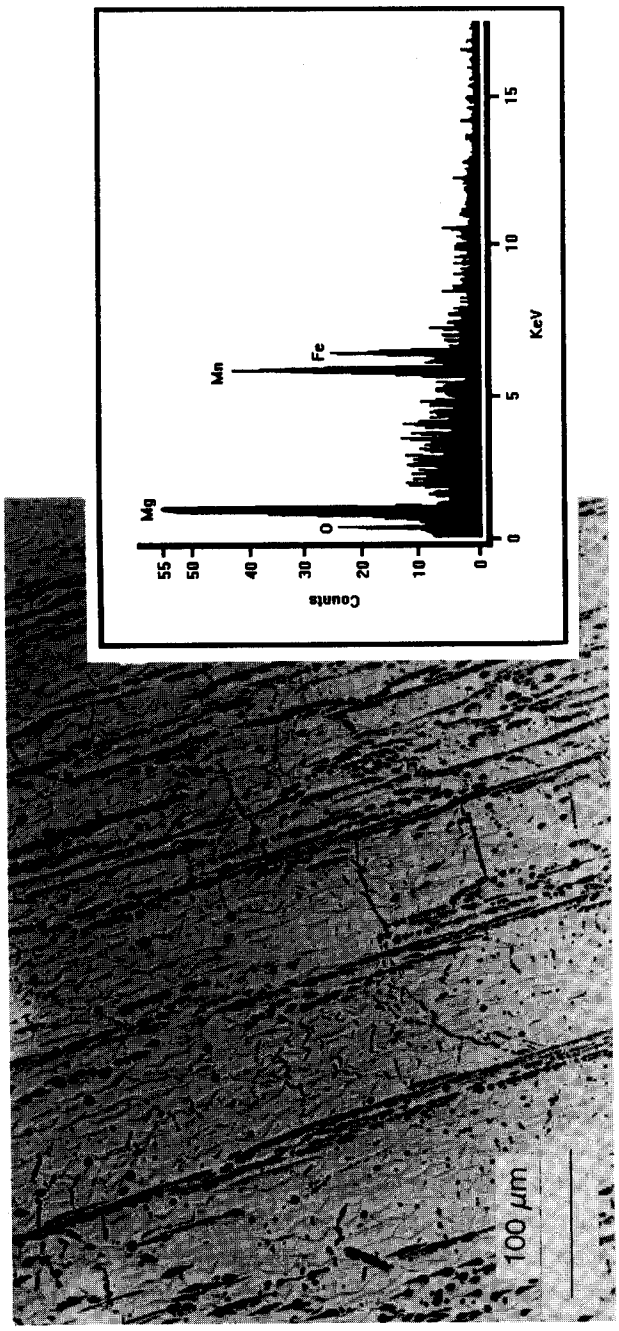

Fig. 6a: Microstructure obtained from an anode cooled in air (400°C/28.8 Ks). Columnar-type microstructure with a substructure inside the columnar grains with fine precipitates. The EDAX pattern shows the presence of Fe and Mn in these fine precipitates.

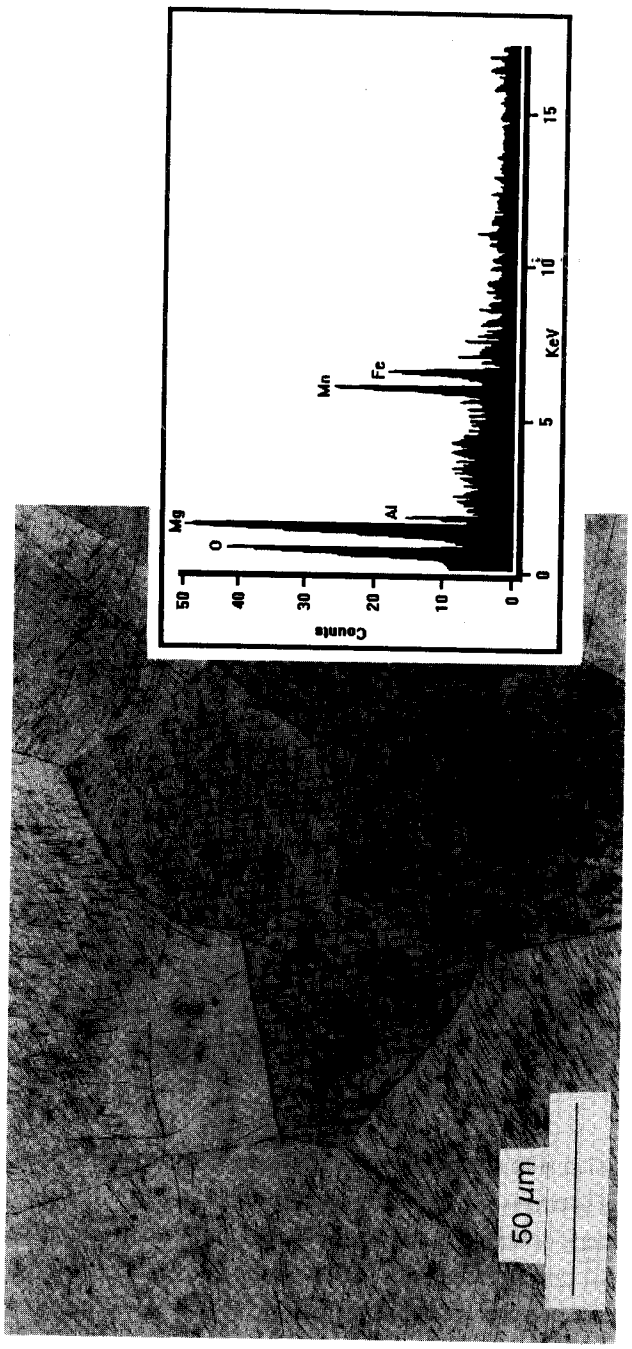

Fig. 6b: Microstructure obtained after the anode was aged (300°C/28.8 Ks). The microstructure observed is needle-like associated wsith fine precipitates finely distributed in matrix. EDAX pattern shows the presence of Al, Mg, Fe and Mn in the fine particles.

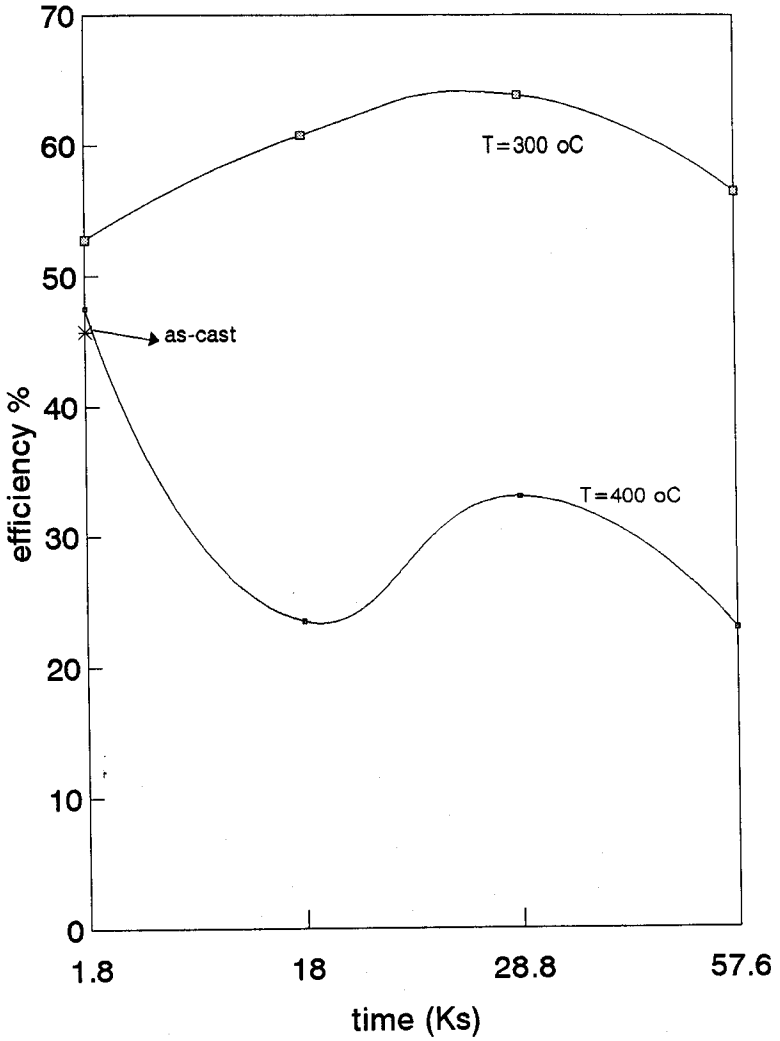

Fig. 7: Graph showing the current efficiency as a function of treatment time for the two ageing treatments (300 and 400°C).

form a stable passive film in certain types of electrolyte, and there is a lack of galvanic action between Mg and Al in Mg-alloys.

The low efficiencies were related to the formation of insoluble particles of Fe-Mn (Fe-rich) that together with the Mn segregated as a second phase, observed directly on samples cooled in air and/or furnace. These precipitates and segregates are not uniformly distributed: in some places the Mn was

Table VI
Chemical composition of magnesium anode.

Element	Anode tested, % weight	Galvomag*, % weight
Al	0.0113	0.01 max.
Cu	0.0015	0.02 max.
Fe	0.020	0.03 max.
Ni	0.0018	0.001 max.
Mn	0.9835	0.5 - 1.3
Mg	difference	difference

Electrochemical Efficiency	51.2 %	> 50 %

segregated and in other regions only the Fe-Mn particles were observed on the grain boundaries. It is possible that during the corrosion test the Fe-Mn particles act as local galvanic microcells of a strong cathodic nature. It has been reported /12/ that this may induce granular corrosion, due to the attack that is concentrated in the regions of the grains next to the boundaries.

Almost all the anodes after the ASTM tests showed non-uniform corrosion when viewed with the naked eye or under low magnification. The surface of these specimens was observed more closely. Figure 8a is a SEM photomicrograph showing the anode in the as-cast condition after ASTM test. Corrosion of Mg occurs preferentially in regions rich in second phase often subject to localized segregation, elemental depletion or precipitation. Corrosion in these regions is by pitting, forming a step-like pattern. The pits were quite deep and in many cases showed cracks at their base. Figure 8b shows the surface appearance of an anode heat treated (aged 400°C, during 18 Ks), with a very low efficiency (27.5%). It can be observed that the corrosion pattern is almost similar to the pattern showed for the as-cast anode (Figure 5a), i.e. pitting, forming a step-like pattern. Figure 8c is a heat treated anode (furnace cooled, 400°C/28.8 Ks), and shows a pitted region. Such pits are very deep and certainly indicate accelerated non-uniform corrosive attack at high energy locations (i.e. grain boundaries and/or precipitates). Figure 8d, shows uniform corrosion attack, which was found in the heat treated anodes (aged 300°C, during 28.8 Ks), with high efficiencies (i.e. 60% or more). This pattern was obtained inside the pits uniformly distributed along the anode. This uniform attack was observed in

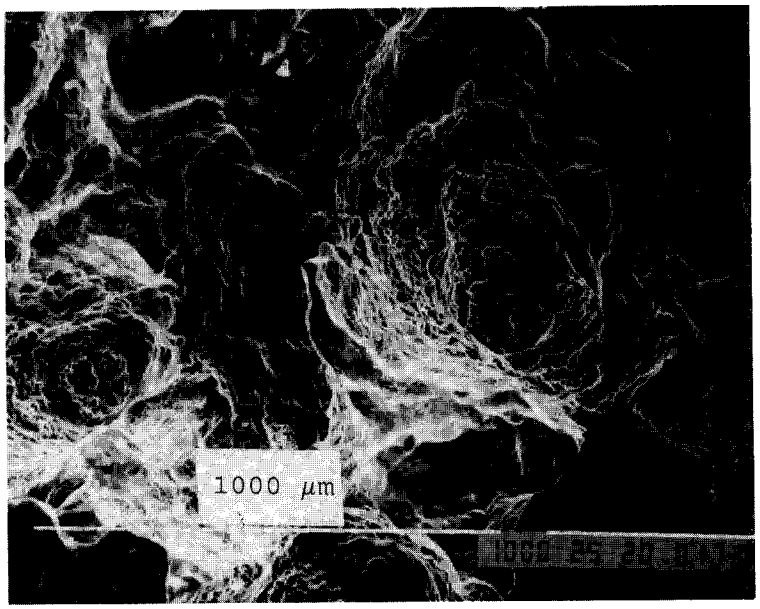

Fig. 8a: SEM micrograph showing the anode in the as-cast condition after the ASTM test. It can be observed that the corrosion is by pitting.

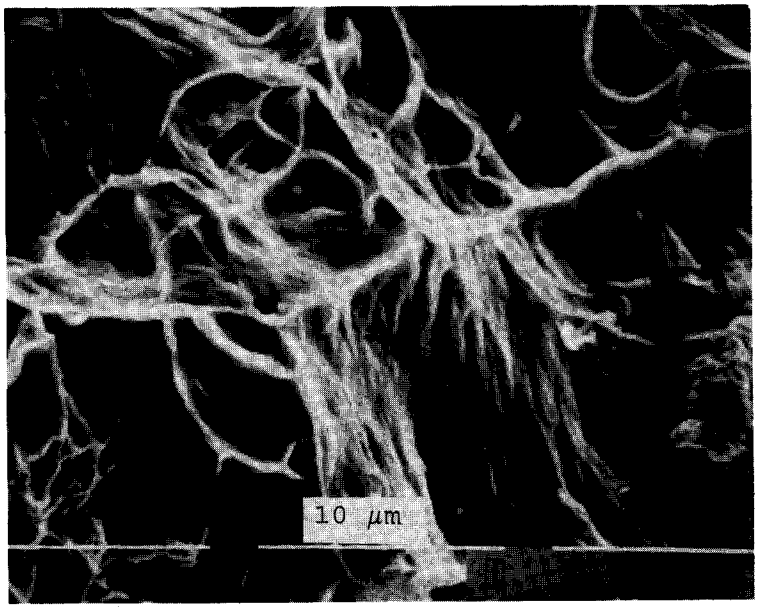

Fig. 8b: SEM micrograph from the anode aged (400°C/18 Ks) after the test. It shows a similar corrosion pattern as Figure 5a.

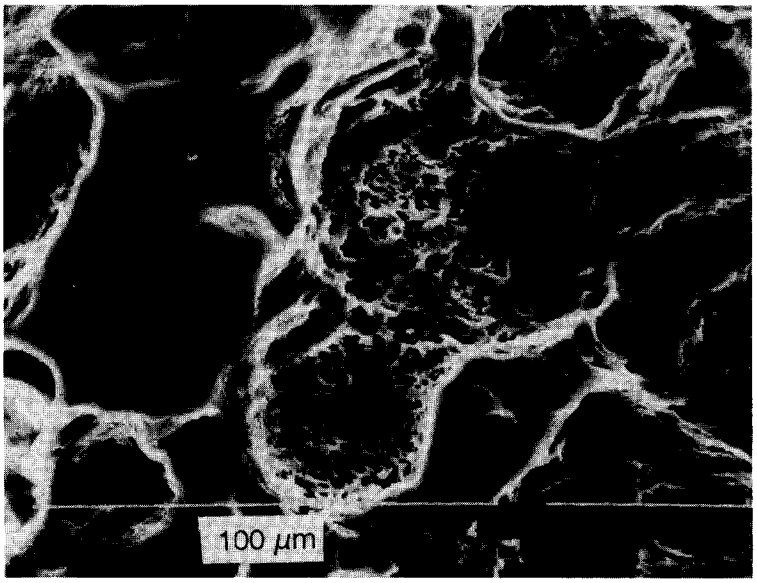

Fig. 8c: SEM micrograph obtained from the anode furnace cooled (400°C/ 28.8 Ks). The corroded surface shows pits indicating an accelerated non-uniform corrosion.

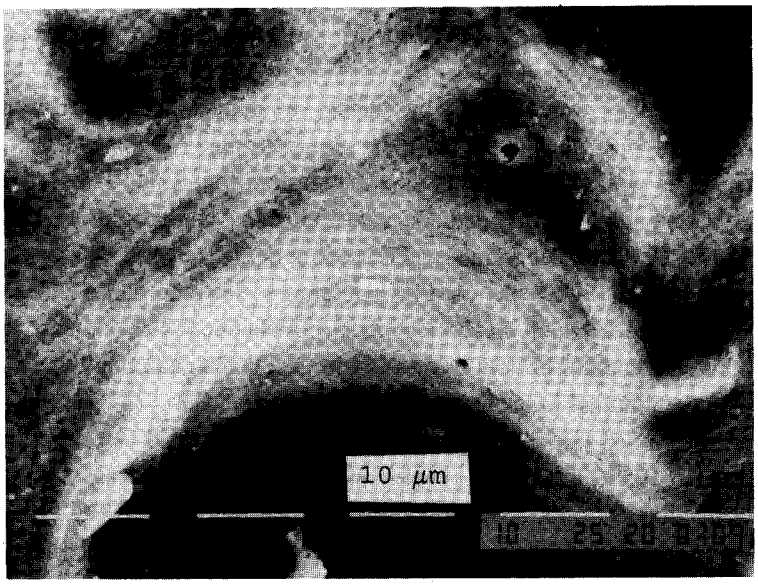

Fig. 8d: SEM micrograph showing the anode aged (300°C/28.8 Ks) after the ASTM test. A uniform corrosion pattern can be observed.

almost all the anodes heat treated with high efficiencies. A few spherical particles were found, roughly 1μm in diameter. Such particles were rich in Fe-Mn and widely distributed over the surface, inducing a relatively uniform attack.

From the results obtained in this work and considering recent reports /13,14/, values higher than 50% of efficiency were obtained. These values are directly related to the microstructure/cooling rate (see Tables IV and V) of the Mg-anodes. For example, according with the particle and/or grain size measured in the as-cast anodes, the cooling rate varied from 10^3 °K/s (roughly 5μm in particle size) to 10^2 °K/s (roughly 10μm in particle size), meaning a considerable refinement of the microstructure compared with the as-cast anodes that have particle and/or grain size of about 100 μm or more. On the other hand, impurities such as Cu and Ni, and second-phase particles rich in Fe and Al were partially dissolved by the heat treatment (aged). This caused an increase in their efficiency and overall uniform corrosion rather to localized corrosion (pitting).

Electrochemical Evaluation

Experimental Procedure

The specimen preparation and experimental procedure were made following the methods as described in the two standards previously mentioned /1,2/.

Measurements were made by using a standard three-electrode configuration with the working electrode controlled at the measured potential. The working electrode was a magnesium rod, Table I, machined from a Galvomag[1] commercial anode, whose chemical composition is shown in Table VI. Five samples were tested according to the standard. A saturated calomel electrode (SCE) was used as a reference electrode and a piece of steel pipe, Table I, which served also as electrochemical cell (cathode test pot), being the counter or auxiliary electrode. Applied signal amplitude was 10 mV in the nominal frequency range of 10 KHz to 1 Hz.

Each machined test specimen was rinsed with water and acetone, dried in an oven at 105°C for 30 min., cooled and weighed to the nearest 0.1 mg.

Electrochemical impedance was measured by using a CAPCIS CV 2001 Frequency Response Analyser (FRA), and a CAPCIS March Electro-

[1] Trademark of the Dow Chemical Company.

chemical Interface was employed to apply the desired potential. All the equipment was controlled by means of a PC XT computer, which used Sheila software /15/.

The samples were held galvanostatically at 0.039 mA/cm^2 until E.I.S. testing, at which time the samples were held potentiostatically during the time of the test. Closed circuit test specimen potential was obtained daily, before and after E.I.S. testing.

X-ray diffraction analysis of the corrosion products formed on the magnesium anode at the end of the test was performed on Siemens D-500 equipment.

Results and Discussion

Electrochemical Impedance Spectroscopy (E.I.S.) measurements were used to monitor the corrosion process on the magnesium anode daily for the 14 days of test. The anode current density was 0.039 mA/cm^2 throughout the test, according to ASTM G 97-89 /1/; the reading did not vary with time.

The potential of the magnesium anode was measured daily, with a change from -1610 mV to -1680 mV vs. SCE after 14 days. This behaviour is normal in these types of tests, and no further information can be obtained from this slight cathodic shift.

Figure 9 gives the characteristic impedance spectra obtained during the time when the magnesium anode was immersed in the solution for 14 days at 20^{o}C, always showing two loops. To interpret the impedance results, a model was established /16/, which includes the electrolyte resistance, the parts of the impedance corresponding to the corrosion product film (hydroxide layer) formed and the impedance of the interface.

The spectra analysis shows the capacitance C_{po} of a corrosion porous layer in the high frequency region, the capacitance of double layer C_{dl} in the low frequency region, the resistive component R_{po} of the corrosion porous layer in the frequency range between 100 and 1000 Hz and the resistance of charge transfer reaction R_t in the low frequency region. In order to interpret the impedance diagrams, equivalent circuit models were used. The behaviour of the magnesium/electrolyte interface can be described by the proposed model with the electric equivalent circuit that corresponds to porous film model or Two Layer Model (TLM) /16/, which has been used to reproduce with success all the impedance spectra obtained. According to this model, the impedance diagram might bring into view two semicircles. The high frequency semicircle is usually attributed to the porous film, whereas

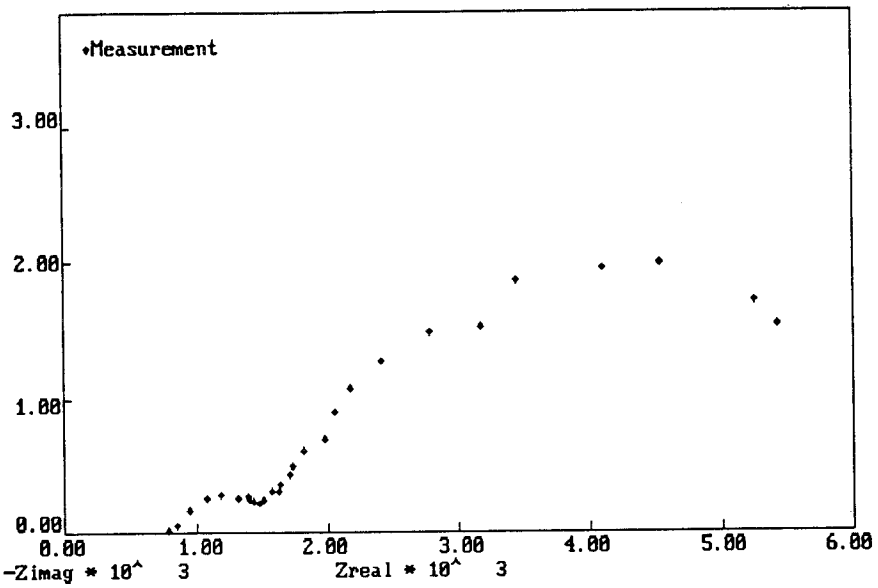

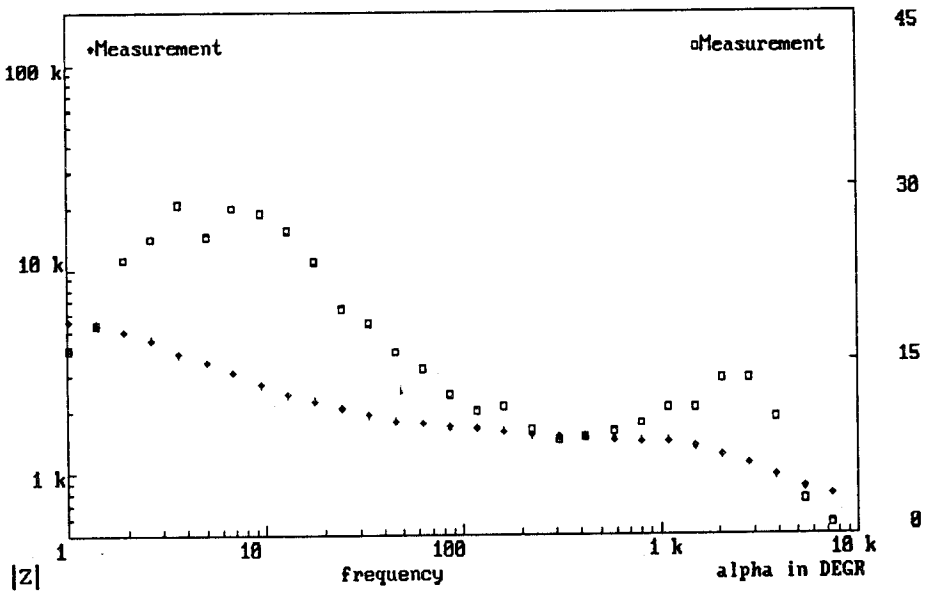

Fig. 9: Typical impedance diagram (Nyquist and Bode representation) of magnesium galvanic anode recorded during the ASTM test.

the lowest frequency semicircle corresponds to the charge transfer reaction or faradaic process.

Boukamp equivalent circuit software /17/ was employed to determine the equivalent electric circuit. In Figure 10 one can see, in terms of the Bode and Nyquist plot, the good simulation obtained.

The capacitance of the corrosion porous layer C_{po} decreases with time, Figure 11, whereas both resistances, R_{po} and R_t, increase with time, Figure 12. This increase in protection with immersion time probably provide evidence for the existence of a protective layer over the magnesium surface, $Mg(OH)_2$.

The capacitance C_{po} of the layer can be described by the following formula:

$$\frac{C}{A} = \varepsilon\varepsilon_0 \frac{1}{d}$$

where ε is the dielectric constant, ε_0, the permittivity in free space (8.854×10^{-12} F/m), C/A, the capacitance per unit area and d, the thickness. Thus, as the thickness of the $Mg(OH)_2$ increases, C is expected to decrease, as one can see, for the C_{po} value, Figure 11. One possible way to estimate the thickness of the film is by making use of the above relationship. As a result of using a value of C/A of 0.2×10^{-6} F/cm^{-2} and ε of 5 to 20 (the range of values for a number of oxidised metal solids) /18/, a film with thickness d of the order of 221.4 to 885.4 Å results.

Since the resistance of a film is proportional to its resistivity and thickness, an increase in R_{po} is interpreted to mean that the passivation of the $Mg(OH)_2$ layer increases with the time of immersion.

The analysis of the corrosion products formed on the magnesium anode and precipitated in the solution was made by X-ray diffraction analysis /16/. A visual and microscopic inspection of the magnesium electrode did not show any localized corrosion after the test.

Under the Mexican standard conditions /2/, it was not possible to demonstrate the $Mg(OH)_2$ - film formation. The impedance diagrams showed, in all cases, the presence of only one semicircle. After the end of the test, the corresponding visual and microscopic inspection of the magnesium electrode showed a very localised corrosion.

By the results obtained, the magnesium anode did not corrode locally in the ASTM test, and charge transfer is occurring uniformly underneath the

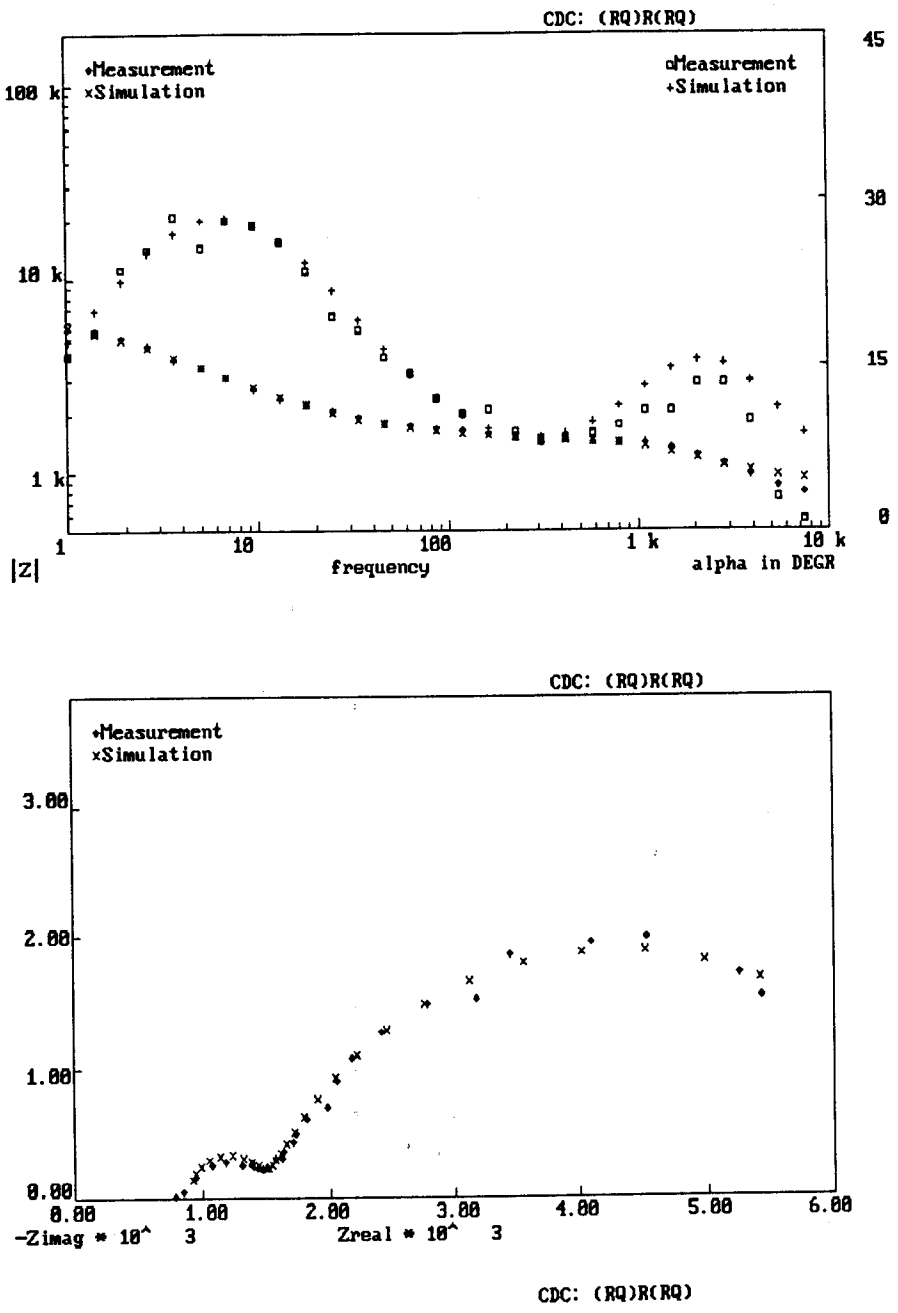

Fig. 10: Magnesium impedance diagrams simulation (Bode and Nyquist representation) by means of Boukamp /17/ software.

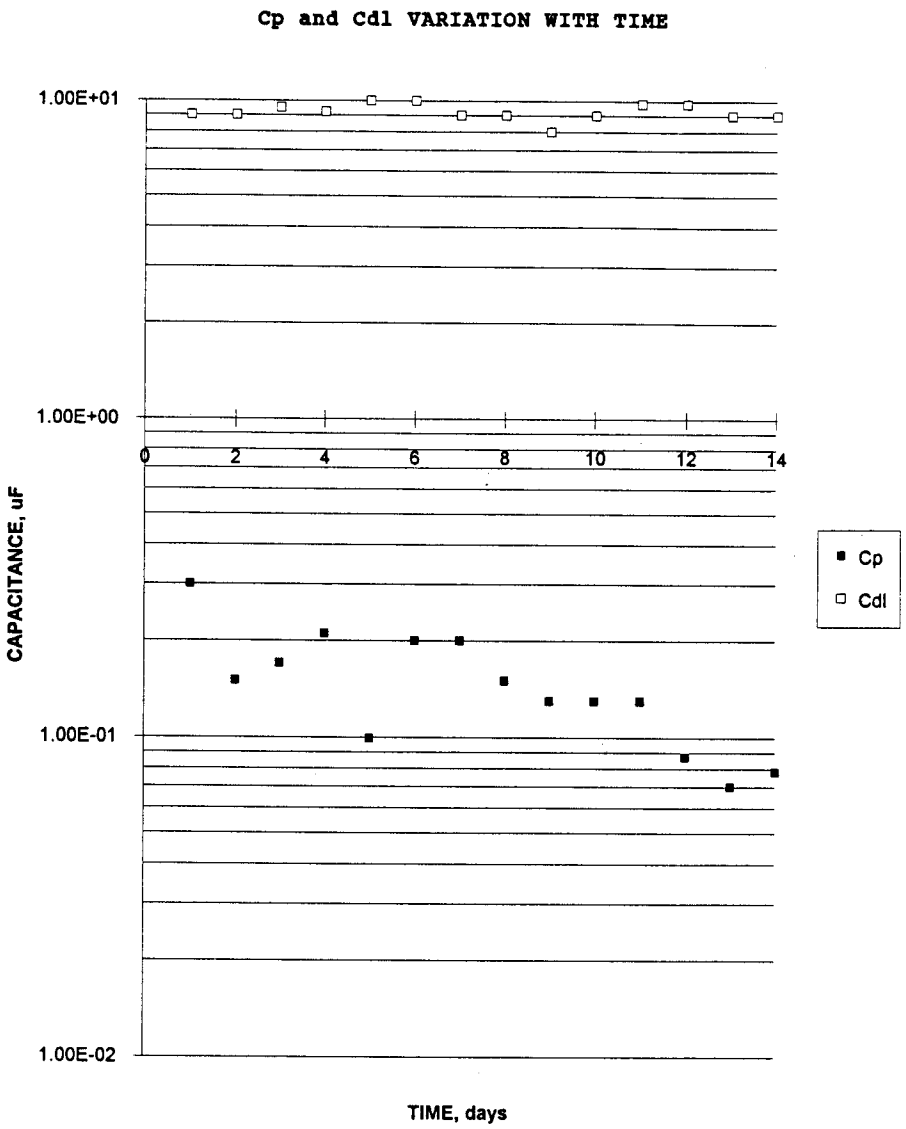

Fig. 11: Film and double layer capacitance variation with immersion time.

oxide. In this case, the physical arrangement of the circuit elements seems to be consistent with the model presented /16/, in which a series arrangement of the film elements, R_{po} and C_{po} and $C_{dl}R_t$ time constant would be representative of the interface under study. In the artificial sea water, where

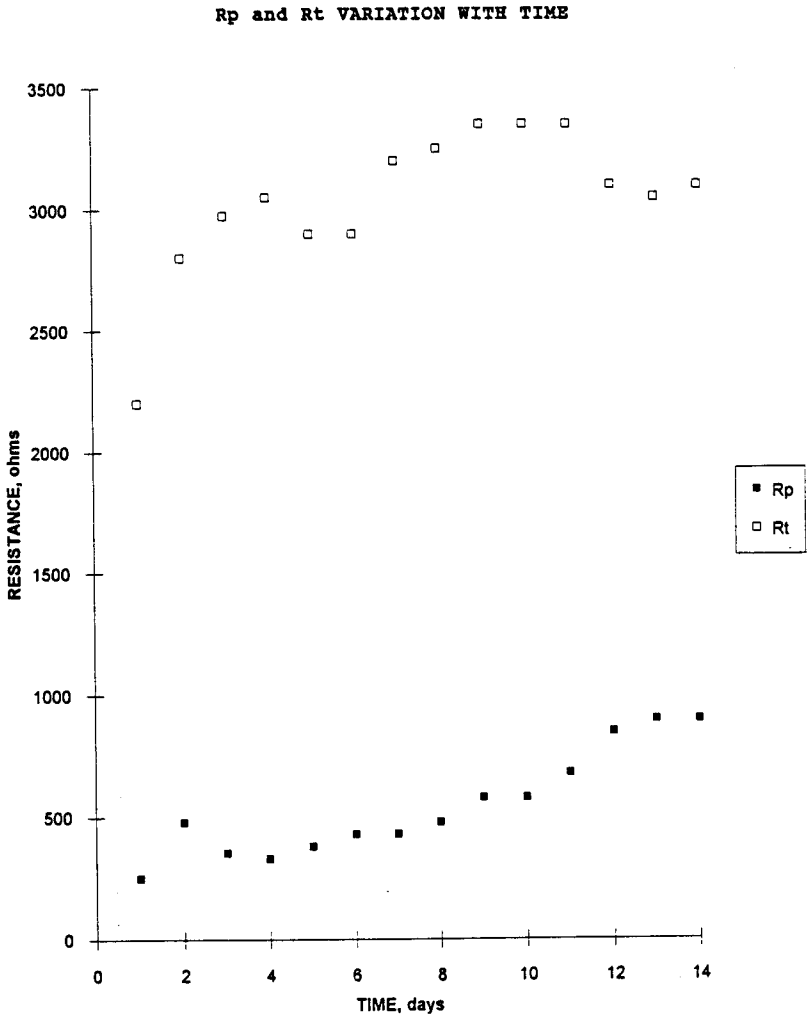

Fig. 12: Film and charge transfer resistance variation with immersion time.

pitting is observed, the model representative of the interface consists of, but it is unclear why only one time constant is observed in this condition.

The Galvomag[2] anode, containing high purity magnesium with 0.9 - 1.2 % added manganese and controlled impurities, has a solution (open circuit)

[2] Trademark of the Dow Chemical Company.

potential of -1.68 V vs. SCE. From the factors responsible for the low current efficiency and the potential of the magnesium anode, which is nobler than the theoretical solution potential, we may say that the anolyte chemistry (changes in anion and cation concentration which occur close to the dissolving magnesium surface) can be a contributing factor in the manifestation of these properties. A $Mg(OH)_2$ accumulation around the anode is necessary in order to stabilize the pH between 9.5 and 10.5 /19/. In fact, the best performance of the magnesium anodes was achieved at these pH values. At a pH lower than 9.5, a cathodic film is formed on impurities, which isolates them from the environment, retarding auto corrosion. Chloride ions break this cathodic film formed on anodic impurities with an increase in auto corrosion. Chlorides are usually corrosive even in solutions having pH values above that required to form magnesium hydroxide.

The precipitation of $Mg(OH)_2$ film, with properties of low solubility and high protection, allows it to have such resistance to water that it can be used in practice. pH changes adjacent to the high purity Mg+Mn anode in a 0.1 N NaCl solution saturated with $Mg(OH)_2$ over an anode current density range of 0.15 to 1.5 mA/cm^2 (1 to 10 $mA/inches^2$) /3/ show that the anolyte rapidly becomes alkaline attaining a pH slightly in excess of 11. This activity probably reflects the attainment of equilibrium

$$Mg^{2+} + 2OH^- \Leftrightarrow Mg(OH)_2 \qquad K_{sp} = 1.2 \times 10^{-11}$$

The precipitation of the $Mg(OH)_2$ takes place on or very close to the anode surface. Upon decreasing the applied anode current density, the chloride ion concentration almost instantaneously decreased, as did the pH.

The film repairing process is mainly due to the $Mg(OH)_2$ - formation at anode/solution interface, whereas the breaking process can be considered simply as the generation of magnesium soluble salts at the interface. This can damage the film in two ways. First, because of the common ion effect, acidity increases as the magnesium soluble salt concentration increases, with a consequent solubility enlargement in $Mg(OH)_2$. Second, high concentrations of magnesium salts such as chlorides can damage the film, modifying it by means of incorporation of these salts between the $Mg(OH)_2$ strata, thus increasing the space between them.

GENERAL CONCLUSIONS

This investigation led to the processing of Mg anodes and, from the practical point of view, values higher than 50% efficiency which are relevant for conventional applications.

These values of efficiency are directly related to the microstructure obtained during the chill casting practice of the magnesium sacrificial anode.

Impurities such as copper and nickel remained in solid solution and second phase particles rich in iron were partially dissolved by heat treatment, which results in an increase in their efficiency and a more uniform corrosion pattern rather that pitting.

Using specific heat treatments the efficiency of the Mg anodes was improved, which made it possible to control the amount and size of the precipitates and of the second phase particles localized at grain boundaries and inside the matrix.

Lower anode efficiency was related to the presence of Mn rich second phase particles where corrosion occurs along a narrow region in the grain boundaries.

In order to produce high efficiency of Mg-anodes it is necessary to control the impurities that are uniformly distributed in solid solution, and other microstructural parameters such as grain size. The solution could be to use alternative casting processes /14/ and heat treatments.

Some evidence has been collected to demonstrate that from the two different standards employed in the testing of the magnesium anodes, only under the ASTM G-97-89 standard conditions was it possible to assure the presence of $Mg(OH)_2$ film throughout the test.

ACKNOWLEDGMENTS

One of the authors (J.G.) would like to acknowledge the financial support of the Direccion General de Asuntos del Personal Academico (DGAPA), UNAM, for this research (project num. IN 103791). The technical support of O. Flores, J.L. Albarran and A. Gonzalez is acknowledged.

REFERENCES

1. "Standard Test Method for Laboratory Evaluation of Magnesium Sacrificial Anode Test Specimens for Underground Applications" ASTM G 97-1989. *Annual Book of ASTM Standards,* Volume 03.02. pages 377-380. Philadelphia, 1989.
2. "Anodos de magnesio empleados en proteccion catodica". NOM K 109-1977. Direccion General de Normas Industriales. Mexico D.F., 1977.
3. C.F. Schreiber, "Sacrificial Anodes" in *Cathodic Protection - Theory and Practice.* Crest Hotel, Walsgrave, Coventry, England, 1982.
4. H.A. Robinson and P.F. George, *Corrosion,* **10** (6), 182 (1954).
5. H.A. Robinson, *Trans. J. Electrochem. Soc.*, **90**, 485 (1946).
6. J.D. Hanawalt, C.E. Nelson and J.A. Peloubet, *Corrosion Studies of Magnesium Alloys,* Metals Technology, September, 1941.
7. O. Osborn and H.A. Robinson, *Corrosion* **8** (4), 114 (1952).
8. J.B. Besone, R.A. Suarez and S.M. De Micheli, *Corrosion* **37** (9), 533 (1981)
9. R. Tunold, *Corrosion Sci.*, **17**, 533 (1977).
10. H. Jones, *J. Mater. Science*, **19**, 1043 (1984).
11. A. Joshi and R.E.Lewis, in *Advances in Mg Alloys and Composites,* eds. H. Paris and W.H. Hunt, The Met. Soc., AIME, Warrendale, PA, 1989, p.89.
12. K.G. Adamson, *Corrosion,* 2nd ed., Editor L.L. Shreir, 4: 86 - 4: 101, Newnes-Butterworth, London, 1976.
13. J.A. Juarez-Islas, J.Genesca and R. Perez, *JOM,* September (1985) p.42.
14. J.A. Juarez-Islas, L. Martinez and J. Genesca, Corrosion'93, Paper No.536. NACE, Houston, 1993.
15. SHEILA. Capcis March. Manchester.
16. J. Genesca, L. Betancourt and C. Rodriguez, *Corrosion* **52** (7), 502 (1996).
17. B. Boukamp, *Equivalent Circuit Software.* University of Twente, 1993.
18. *Handbook of Physics and Chemistry,* 59th ed. R.C. Weast (Ed.), 1978; pp. E58-E61.
19. C.F. Schreiber, in *Secondo corso di aggiornamento sulla protezione catodica,* CLUP, Milan 1984, page 85.